33rd Annual International Conference of the IEEE EMBS
Boston, Massachusetts USA, August 30 - September 3, 2011

A Two-Stage Cascade Nonlinear Dynamical Model of Single Neurons for the Separation and Quantification of Pre- and Post-synaptic Mechanisms of Synaptic Transmission

Ude Lu, *Student Member*, Shane M. Roach, *Student Member*,
Dong Song, *Member*, and Theodore W. Berger, *Fellow*, *IEEE*

***Abstract*—Neurons receive pre-synaptic spike trains and transform them into post-synaptic spike trains. This spike train to spike train temporal transformation underlies all cognitive functions performed by neurons, e.g., learning and memory. The transformation is a highly nonlinear dynamical process that involves both pre- and post-synaptic mechanisms. The ability to separate and quantify the nonlinear dynamics of pre- and post-synaptic mechanism is needed to gain insights into this transformation. In this study, we developed a Volterra kernel based two-stage cascade model of synaptic transmission using synaptically-driven intracellular activities, to which broadband stimulation conditions were imposed. The first stage of the model represents the pre-synaptic mechanisms and describes the nonlinear dynamical transformation from pre-synaptic spike trains to transmitter vesicle release strengths. The vesicle release strengths were obtained from the intracellularly recorded excitatory post-synaptic currents (EPSCs). The second stage of the model represents the post-synaptic mechanisms and describes the nonlinear dynamical transformation from release strengths to excitatory post-synaptic potentials (EPSPs). One application of this cascade model is to analyze the pre- and post-synaptic mechanism change induced by long-term potentiation (LTP). This future application is expected to shed new light on the expression locus of LTP.**

I. Introduction

All cognitive functions performed by the brain, e.g. learning, memory, recognition, and decision making, are processed stage by stage with its elementary units, neurons. Neurons receive multiple pre-synaptic spike trains and transform them into a post-synaptic spike train. Any information processed by neurons is encoded in the spike-train to spike-train temporal transformation [1, 2]. To understand this temporal transformation is fundamental to unravel the way brain works.

The neuron spike train to spike train transformation is a highly nonlinear dynamical process involving both pre- and post-synaptic mechanisms. The biological processes include (but are not limited to) calcium influx in pre-synaptic terminal, residual calcium dynamics, transmitter vesicle release, kinetics of voltage-dependent ionic channels, dendritic and somatic integrations, and spike generation. The ability to separate and quantify the nonlinear dynamics of pre- and post-synaptic mechanisms is needed to further our understanding to the biological mechanisms underlying the neuron spike train to spike train transformation.

In this study, we developed a two-stage cascade model to describe the nonlinear dynamics of both pre- and post-synaptic mechanisms (Fig. 1). In order to collect the requisite information-rich input-output datasets, the recorded neurons were stimulated pre-synaptically using broadband random interval trains (RITs). The stimulations are all-or-none electrical pulses mimicking action potentials. The broadband RITs elicit biologically plausible processes in both pre- and post-synaptic regions. Whole-cell patch-clamp was utilized to record excitatory post-synaptic currents (EPSCs) and excitatory post-synaptic potentials (EPSPs).

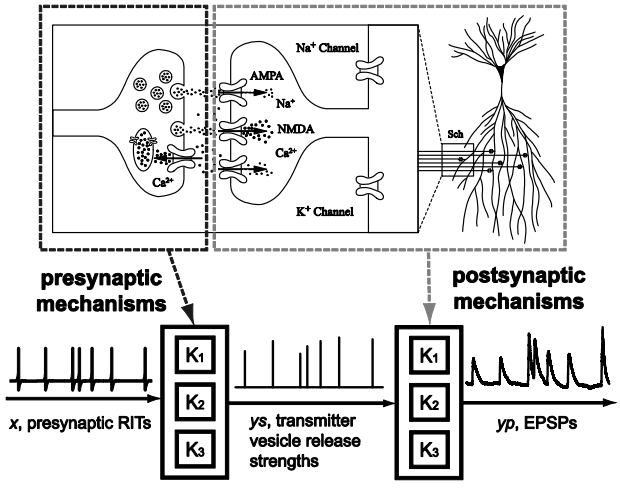

Fig. 1. Model structure of the two-stage cascade model.

Both stages of the model are developed using third-order Volterra kernels to describe the transformation from the input to the output. The first stage of the model represents pre-synaptic mechanisms and describes the nonlinear

Manuscript received March 26, 2011. This work was supported by NSF (USC Biomimetic MicroElectronics Engineering Research Center), DARPA (USC REMIND Program), NIBIB (USC Biomedical Simulations Resource), and ONR (N00014-10-1-0685).

Ude Lu is with the Department of Biomedical Engineering, University of Southern California, Los Angeles, CA 90089 USA (phone: 213-740-8063; fax: 213-740-8061; e-mail: ulu@usc.edu).

Shane M. Roach is with the Department of Neuroscience, University of Southern California, Los Angeles, CA 90089 USA (e-mail: shaneroa@usc.edu).

Dong Song is with the Department of Biomedical Engineering, University of Southern California, Los Angeles, CA 90089 USA (e-mail: dsong@usc.edu).

Theodore W. Berger is with the Department of Biomedical Engineering, University of Southern California, Los Angeles, CA 90089 USA (e-mail: berger@bmsr.usc.edu).

dynamical transformation from pre-synaptic spike trains to transmitter vesicle release strengths. The second stage of the model represents post-synaptic mechanisms and describes the nonlinear dynamical transformation from vesicle release strengths to EPSPs.

To conduct this research, it is critical to estimate vesicle release strengths from the recorded EPSCs. EPSC is a mixture of the nonlinear dynamics of both pre-synaptic vesicle release mechanism and post-synaptic glutamate-receptor channel mediated current dynamics. In this study, the isolation of the vesicle release mechanism is achieved by deconvolving EPSC recordings with an averaged isolated EPSC waveform observed in the same EPSC recordings (see more details in MATERIALS AND METHODS, section *B*). This operation is based on the linearity of AMPA receptor channel-mediated ($AMPA_{RC}$-mediated) current dynamics under three experimental conditions: 1) the post-synaptic current responses (i.e., EPSCs) are recorded under voltage-clamp, 2) the stimulation intensity is sufficiently low, so that the Mg^{2+} cannot be expelled from the NMDA receptor channel ($NMDA_{RC}$), and 3) the smallest inter-spike interval in the RITs applied is 10 ms, so that the nonlinearity due to $AMPA_{RC}$ desensitization is reduced.

II. MATERIALS AND METHODS

A. Electrophysiology

Hippocampal slices (400 μm thick) were prepared from young adult Sprague-Dawley rats (male, four-week-old) with standard procedures in iced cutting (sucrose) solution. The connection between CA3 and CA1 was surgically disrupted to reduce spontaneous activities in CA1 neurons. Slices were maintained and recorded in artificial cerebral spine fluid (ACSF) at room temperature containing (in mM): NaCl 124, KCl 2.5, NaH_2PO_4 1.25, $NaHCO_3$ 26, Glucose 10, $MgSO_4$ 1, Ascorbic Acid 2, and $CaCl_2$ 2; at pH 7.4 and 295 mOsmol. The perfusion ACSF medium for recordings contained 20uM Picrotoxin.

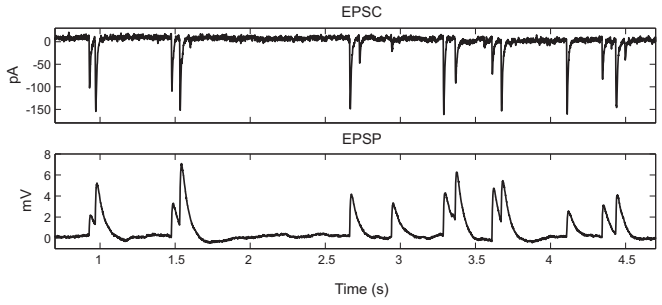

Fig. 2. Representative recordings of EPSCs and EPSPs evoked by the same pre-synaptic RIT stimulation pattern.

A bipolar stimulating electrode was placed on slices based on visual cues as to activate Schaffer collaterals in the CA1 stratum radiatum region. Recording micro-pipette electrodes with a 4 MΩ tip resistance were prepared using a standard puller. The internal solution of the recording electrode contained (in mM): K-SO_3 135, HEPES 10, Mg-ATP 2, and Na_3-GTP 0.25; at pH 7.3 and 290 mOsmol. Random-interval EPSCs and EPSPs were consistently evoked using Poisson distributed RITs with a 2 Hz mean frequency (inter-spike interval 10~4500 ms) and recorded either in voltage-clamp or current-clamp mode (see Fig. 2). The stimulation intensity was set as to evoke a 3 mV peak amplitude in an isolated EPSP.

B. Estimating Vesicle Release Strengths from the Recorded Random-Interval EPSCs

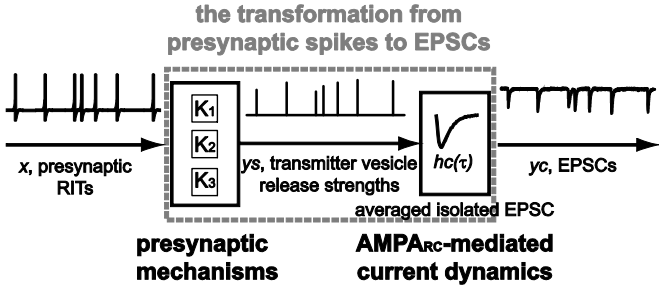

Fig. 3. The transformation from pre-synaptic spikes to EPSCs involves pre-synaptic mechanisms and $AMPA_{RC}$-mediated current dynamics.

The presynaptic RITs (action potentials), $x(t)$, is expressed in a series of impulse responses as follows,

$$x(t) = \sum_{i=1}^{N} \delta(t - t_i) \tag{1}$$

where N represents the total number of action potentials and t_i represents the timing of the i-th action potential. The transmitter vesicle release strength, $ys(t)$, is expressed in a series of impulse responses with varying amplitudes as follows,

$$ys(t) = \sum_{i=1}^{N} A_i \delta(t - t_i) \tag{2}$$

where A_i represents the release strength in response to the i-th pre-synaptic action potential.

Here, we make a reasonable assumption (the validations of this assumption are elaborated in RESULTS section *A*) that, with the experimental conditions applied in this study, the $AMPA_{RC}$-mediated current dynamics is a linear process. Thus, the relationship between EPSC, $yc(t)$, and release strength, $ys(t)$, is expressed as follows,

$$yc(t) = \int hc(\tau) ys(t - \tau) d\tau \tag{3}$$

where $hc(\tau)$ is the linear impulse response of the transformation between $ys(t)$ and $yc(t)$, obtained by averaging all isolated EPSC responses in the same recording. Isolated EPSC is defined as an EPSC having 3000 ms silence period (no stimulation) before and no overlapping EPSC after it (i.e., the first-order EPSC response). With (3), $ys(t)$ can be

obtained by deconvolving $yc(t)$ using $hc(\tau)$.

C. Volterra Modeling of Pre- and Post-synaptic Mechanisms

In Figure 1, the transmitter vesicle release strength $ys(t)$ is expressed with Volterra series as follows,

$$ys(t_i) = A_i = c_1 + \sum_{j=1}^{L} c_2(j) v_j^s(t) + \sum_{j_1=1}^{L} \sum_{j_2=1}^{j_1} c_3(j_1, j_2) v_{j_1}^s(t) v_{j_2}^s(t) \quad (4)$$

where L denotes the number of Laguerre basis functions, c denote Laguerre coefficients, and v_j^s denote the convolutions of Laguerre basis functions and $x(t)$, and is expressed as,

$$v_j^s(t) = \sum_{t-M<t_i<t} b_j(t - t_i) \quad (5)$$

where b denotes Laguerre basis functions and M denotes the memory window.

The EPSP, $yp(t)$, is expressed as follows,

$$yp(t) = c_0 + \sum_{j=1}^{L} c_1(j) v_j^p(t) + \sum_{j_1=1}^{L} \sum_{j_2=1}^{j_1} c_2(j_1, j_2) v_{j_1}^p(t) v_{j_2}^p(t) + \sum_{j_1=1}^{L} \sum_{j_2=1}^{j_1} \sum_{j_3=1}^{j_2} c_3(j_1, j_2, j_3) v_{j_1}^p(t) v_{j_2}^p(t) v_{j_3}^p(t) \quad (6)$$

where c are Laguerre parameters and v_j^p are convolutions of $ys(t)$ and Laguerre basis functions, $b_j(t)$, expressed as follows,

$$v_j^p(t) = \sum_{\tau=0}^{M} b_j(\tau) ys(t - \tau) \quad (7)$$

All c in (4) and (6) are estimated using the least-squares method [3].

D. Reconstructions of Volterra Kernels and Response Functions

Volterra kernels of the pre-synaptic mechanism model (first stage) are reconstructed with the estimated Laguerre coefficients c in (4) as follows,

$$k_1 = c_1 \quad (8)$$

$$k_{i,2\le i\le 3}(m_1, ..., m_i) = \sum_{j_1=1}^{L} ... \sum_{j_{i-1}=1}^{L} c_i(j_1, ..., j_{i-1}) b_{j_1}(m_1) ... b_{j_{i-1}}(m_{i-1}) \quad (9)$$

where m represents the inter-spike interval (ISI). And $k_1=c_1$ is a scalar. Volterra kernels of the post-synaptic mechanism model (second stage) are reconstructed with the estimated Laguerre coefficients c in (6) as follows,

$$k_{i,1\le i\le 3}(\tau_1, ..., \tau_i) = \sum_{j_1=1}^{L} ... \sum_{j_i=1}^{L} c_{k_i}(j_1, ..., j_i) b_{j_1}(\tau_1) ... b_{j_i}(\tau_i) \quad (10)$$

Response functions (see Fig. 5) can be calculated from the Volterra kernels k to provide intuitive physiological interpretations in terms of single-pulse, paired-pulse, and triple-pulse effects [3, 4].

III. Results

A. The Linearity of $AMPA_{RC}$-Mediated Current Dynamics

By expressing the relationship between $yc(t)$ and $ys(t)$ in a convolution form as (3), we are assuming that the $AMPA_{RC}$-mediated current dynamics is a linear process with an impulse response being the averaged isolated EPSC $hc(\tau)$. This is a key assumption in this report and needs to be verified.

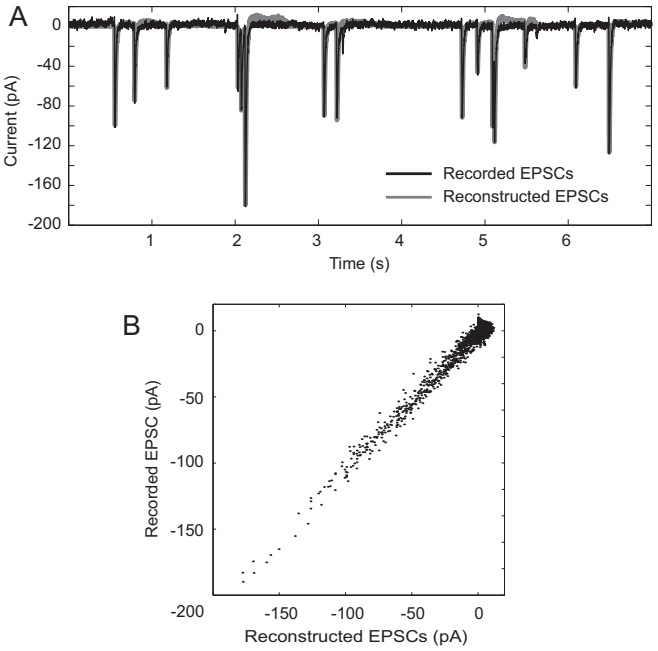

Fig. 4. The reconstructed EPSCs produced by convolving $ys(t)$ and $hc(t)$. Overlapping (A) and scatter plot (B) of the recorded EPSCs and reconstructed EPSCs.

First, in order to make sure that the EPSCs recorded are $AMPA_{RC}$-mediated instead of a mixture of $AMPA_{RC}$ and $NMDA_{RC}$. Two experimental manipulations applied to ensure this: 1) EPSCs were recorded using voltage-clamp at the resting potential which keeps most $NMDA_{RC}$ inactivated, because $NMDA_{RC}$ needs about 15 mV depolarization from the resting potential to expel the Mg^{2+} ion from its mouth to be activated; 2) stimulation intensity was set as the peak value of an isolated EPSP is about 3 mV, so that in the case that patch-clamp cannot provide sufficient control over some distal synapses (the space-clamp issue), $NMDA_{RC}$ still remains inactivated. Second, we need to reduce the potential $AMPA_{RC}$ nonlinearity in the recorded EPSCs. The potential nonlinearity is primarily caused by the desensitization of $AMPA_{RC}$ during repetitive stimulations which has been

reported to have a time constant of 10 ms [5]. According to this, the smallest ISI in the applied RITs is set to 10 ms, so that the most effective time range (0~10 ms) of $AMPA_{RC}$ desensitization is not included. Also, the Schaffer collateral-CA1 synapses have a relatively low (~30%) release probability in response to pre-synaptic action potentials [6]. Using electrical stimulation results in only ~10% of the accessible synapses to be activated twice in a two consecutive stimulation, and thus results in an even weaker desensitization effect beyond 10 ms ISI [7].

Results in Fig. 4 show that the $AMPA_{RC}$-mediated nonlinearity is indeed negligible in the recorded EPSCs. This is indicated in the almost perfect overlap between the recorded EPSCs and reconstructed EPSCs (see Fig. 4A), where the reconstructed EPSC is obtained by convolving $ys(t)$ and $hc(\tau)$. The scatter plots of the recorded and reconstructed EPSC are almost perfectly dotted on the diagonal (see Fig. 4B). Both figures validate the assumption that of $AMPA_{RC}$-mediated current dynamics is linear, and justifies the practice of estimating the release strengths, *ys*, by deconvolving the EPSC recording using an averaged isolated EPSC observed in itself.

B. Response Functions of Pre- and Post-synaptic Mechanisms

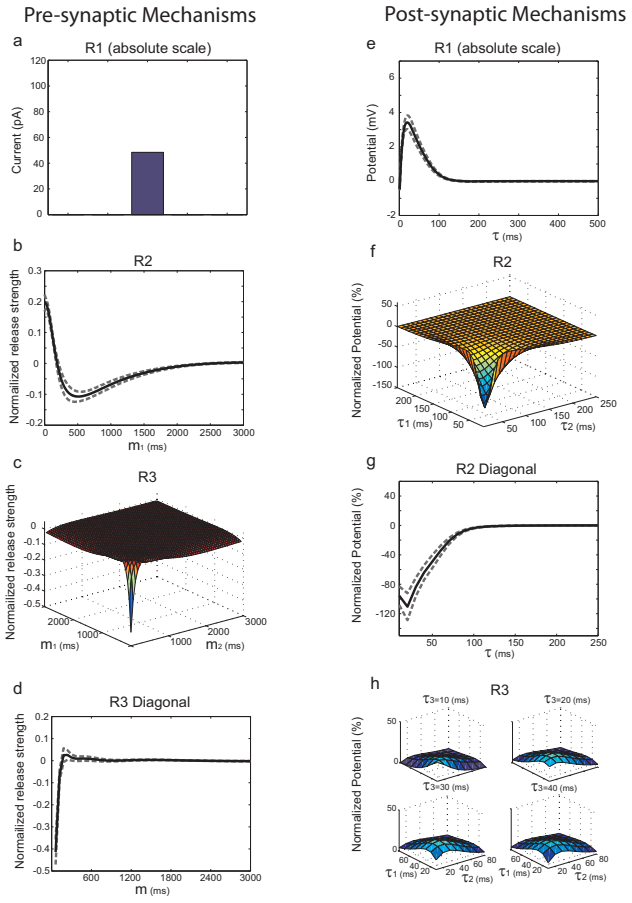

Fig. 5. Response functions of pre-synaptic and post-synaptic mechanisms.

Averaged response functions of pre- and post-synaptic mechanisms are shown in Fig. 5. The general physiological meanings of response functions (either pre-synaptic or post-synaptic mechanisms) are: R1 describes the single-input, linear response; R2 describes the paired-pulse nonlinear response; R3 describes the triple-pulse nonlinear response [3]. In both pre- and post-synaptic stages, the R1 is plotted in absolute value and the R2 and R3 are normalized using the peak value in R1. In pre-synaptic mechanism response functions, *m* represents ISI; in post-synaptic side, τ represents time epoch. The response functions of pre-synaptic mechanisms is one-dimension lower than post-synaptic, because the outputs of the first-stage of the model are scalars (release strengths) and the outputs of the second-stage of the model are continuous waveforms (EPSPs).

IV. Discussion

In this study, we developed a two-stage nonlinear input-output model using Volterra kernels. This two-stage cascade model separates and quantifies both pre- and post-synaptic mechanism nonlinear dynamics, where the first-stage describes the transformation from pre-synaptic spike to transmitter vesicle release strength, and the second stage describes the transformation from the release strength to EPSP.

Long-term potentiation (LTP) refers to the long-lasting strengthening in synaptic connection and has been understood as a fundamental mechanism underlying learning and memory. Whether LTP expression locus is pre-synaptic or post-synaptic remains controversial. This model is expected to provide new evidence to this debate [8, 9].

References

[1] T. W. Berger, *et al.*, "The Neurobiological Basis of Cognition: Identification by Multi-Input, Multioutput Nonlinear Dynamic Modeling: A method is proposed for measuring and modeling human long-term memory formation by mathematical analysis and computer simulation of nerve-cell dynamics," *Proc IEEE Inst Electr Electron Eng,* vol. 98, pp. 356-374, Mar 4 2010.

[2] D. Song, *et al.*, "Nonlinear dynamic modeling of spike train transformations for hippocampal-cortical prostheses," *IEEE Trans Biomed Eng,* vol. 54, pp. 1053-66, Jun 2007.

[3] U. Lu, *et al.*, "Nonlinear dynamic modeling of synaptically driven single hippocampal neuron intracellular activity," *IEEE Transactions on Biomedical Engineering,* vol. 58, 2011.

[4] D. Song, *et al.*, "Parametric and non-parametric modeling of short-term synaptic plasticity. Part I: Computational study," *J Comput Neurosci,* vol. 26, pp. 1-19, Feb 2009.

[5] L. O. Trussell and G. D. Fischbach, "Glutamate receptor desensitization and its role in synaptic transmission," *Neuron,* vol. 3, pp. 209-18, Aug 1989.

[6] K. A. Foster, *et al.*, "Interaction of postsynaptic receptor saturation with presynaptic mechanisms produces a reliable synapse," *Neuron,* vol. 36, pp. 1115-26, Dec 19 2002.

[7] D. Song, *et al.*, "Parametric and non-parametric modeling of short-term synaptic plasticity. Part II: Experimental study," *J Comput Neurosci,* vol. 26, pp. 21-37, Feb 2009.

[8] T. W. Berger and R. J. Sclabassi, "Long-term potentiation and its relation to hippocampal pyramidal cell activity and behavioral learning during classical conditioning," in *Long-term potentiation: from biophysics to behavior*. vol. Neurology and neurobiology, Volume 35, P. W. Landfield and S. A. Deadwyler, Eds., ed, 1988.

[9] U. Lu, *et al.*, "Nonlinear dynamic analyses of single hippocampal neurons before and after long-term potentiation," *Conf Proc IEEE Eng Med Biol Soc,* vol. 2010, pp. 2762-5, 2010.